Orientation of Asymmetric Top Molecules in a Uniform Electric Field: Calculations for Species without Symmetry Axes

Wei Kong*

Department of Chemistry, Oregon State University, Corvallis, Oregon 97331-4003

Jaap Bulthuis

Department of Chemical Physics and Laser Center, Vrije Universiteit, de Boelelaan 1083, 1081 HV Amsterdam, The Netherlands

Received: October 5, 1999; In Final Form: November 30, 1999

Calculations of orientation effects of polar molecules in a uniform electric field are presented for the most general scenario, an asymmetric top molecule with a permanent dipole not parallel to a principal axis. In addition to details of the calculation procedure, including matrix elements of the Hamiltonian, three different treatments of the population distribution of the Stark levels in an electric field are discussed. The adiabatic approach assumes the noncrossing rule for all energy levels as the orientation field increases, the nonadiabatic approach searches for the level with the most similar wave function under field-free conditions to find the population of the Stark level in the field, and the thermal calculation assumes thermal distribution for all of the Stark levels. Among these, the thermal calculation results in the highest degree of orientation, and in high fields, it shows the best agreement with available experimental data in terms of polarization ratios (the ratios of overall excitation probabilities under two perpendicular polarization directions of the laser). By use of cytosine at a rotational temperature of 5 K and adenine at 2 K as model compounds, the thermal calculation suggests that in a field of 50 kV/cm, more than 30% of the molecules should be confined within a 45° cone surrounding the direction of the orientation field, and that if a transition dipole is perpendicular to the permanent dipole, the excitation probability can be enhanced by 50% when the polarization direction of the laser is perpendicular, rather than parallel, to the orientation field. The adiabatic and nonadiabatic calculations yield similar distribution functions of the permanent dipole, both predicting weaker orientation than that of the thermal calculation. According to comparisons of spectroscopic details between the calculations and experiment using the $\pi^* \leftarrow n$ transition in pyrimidine, however, all three calculations agree with the experimental spectra. Further experimental evidence with higher quality spectra is needed for a conclusive statement. Orientation using a uniform electric field is particularly suitable for studies of large systems with small rotational constants: the orientation effect is proven to be determined by the size of the permanent dipole, essentially independent of the orientation of the permanent dipole in the molecular frame. For small molecules, however, this type or orientation is unfavorable, and the resulting orientation is sensitive to the molecular parameters, such as the rotational constants, and the size and direction of the permanent dipole in the molecular frame.

1. Introduction

By use of a uniform electric field, orientation of gas-phase polar molecules and clusters has been achieved in numerous reports.[1−30] This technique relies on the electrostatic interaction between the permanent dipole and the electric field, so it is applicable to linear, symmetric top, and asymmetric top molecules.[31−36] For example, Miller's group has routinely used this technique to separate cofragments from photodissociation of van der Waals clusters,[1−7] Loesch's group and Stolte's group have investigated steric effects in bimolecular collisions from oriented polar molecules,[8−14] Herschbach's group has measured spectroscopy of the "pendular" states,[15−18] and Vigué's group has measured the distribution of molecular axes in oriented ICl from its photofragments.[19−21] We have quantified the effect of this orientation method through the $\pi^* \leftarrow n$ transition in pyrimidine and pyridazine, and used it for studies of photodissociation of stable molecules such as ICN, BrCN, and *tert*-butyl nitrite.[22−28] In addition, we have developed a strategy for the determination of the direction of a transition dipole by observing the polarization dependence of the excitation probability in an oriented system. On the theoretical front, the methodology for the calculation of molecular orientation has been documented in the original papers on this technique,[8,31−35] although only details on linear and symmetric top molecules have been provided. Bulthuis et al. further extended the calculation to orientation of a special group of asymmetric tops, molecules with their permanent dipoles parallel to a principal axis.[36] On this basis, we and Miller's group calculated spectral details in bound-to-bound transitions.[23,25,37] However, no effort has been made so far to extend the calculation to the most general case where the permanent dipole is not parallel to any principal axis. This step of generalization has become imperative due to our recent attempt to extend this orientation technique to investigations of electronic transitions in biologically relevant species: almost all biomolecules are asymmetric tops, and their dipoles are usually not parallel to any principal axis.

A debated topic in the theoretical treatment of the Stark effect is the population in each Stark level under typical experimental

10.1021/jp993549x CCC: $19.00
Published on Web 01/19/2000

conditions.[36,38] Almost all of the reported experiments were performed using collimated molecular beams.[1−29] Supersonically cooled molecules drifted from field-free conditions into the orientation field in a collision-free environment. Boltzmann distributions with appropriate rotational temperatures can be used to describe the rotational population under field-free conditions, but the correlation between the Stark levels and the field-free rotational states is not straightforward. In the adiabatic calculation by Bulthuis et al.,[36] a correlation was established by assuming the noncrossing rule for all energy levels as the molecules move into the Stark field. We and Miller's group,[23,25,37] on the other hand, assumed a thermal population in the Stark field, and the obtained spectral intensity distributions showed reasonable agreement with experimental observations.

In this paper, we present the calculation details for an asymmetric top with its permanent dipole not parallel to a principal axis. We will quantify the effect of molecular parameters, such as the direction of the permanent dipole in the molecular frame and the size of rotational constants, on the molecular orientation in an electric field. Two nucleic acid bases will be used for model calculations: adenine (the least polar base) and cytosine (one of the most polar bases). Three different treatments of the population in the Stark field will be used, including adiabatic, nonadiabatic, and thermal distributions, and the results will be compared with experimental data whenever possible.

2. Calculation Details

This calculation is limited to the case of polar molecules in strong electric fields, and only interactions between molecular rotation and the electric field are taken into account. The coupling between nuclear spin and molecular rotation is overtaken by the coupling of the permanent dipole with the electric field,[38] so complete uncoupling of nuclear spin is assumed.[39]

2.1. Matrix Elements. There are two equivalent approaches to obtain the eigenenergies and eigenfunctions of an asymmetric top in a strong uniform electric field. One natural choice is to project the permanent dipole onto the principal axes of the molecular frame (denoted as the inertial frame) and obtain wave functions describing the distribution of the principal axes in the laboratory frame. The other choice is to define the permanent dipole as the *z* axis of the molecular frame (denoted as the dipole frame), and the resulting wave functions describe the distribution of the permanent dipole. In this calculation, the latter approach is adopted for the convenience in computer programming. A difficulty with this approach, however, is related to the calculation of the inertial matrix: the principal axes are not the axes of the Cartesian coordinate system in the dipole frame. This problem is solved through a unitary transformation from the inertial frame to the dipole frame: once the Hamiltonian matrix $\hat{H}$ in the inertial frame is obtained, the Hamiltonian matrix $\hat{H}'$ in the dipole frame becomes

$$\hat{H}' = D(\theta_m,\varphi_m)^{+}\hat{H}D(\theta_m,\varphi_m) \tag{1}$$

where $D(\theta_m, \varphi_m)$ is a rotation matrix, and θ_m and φ_m are the Euler angles of the permanent dipole in the inertial frame.

Symmetry adapted wave functions $|JKMs>$ in the inertial frame are used as basis functions:[40]

$$|JKMs> = \frac{1}{\sqrt{2}}(|JKM> + (-1)^s|J - KM>) \qquad (K > 0,\ s = 0 \text{ or } 1) \tag{2}$$

where $|JKM>$ are wave functions of a prolate symmetric top and K is the projection of J along the A axis in the inertial frame. The Hamiltonian operator $\hat{H}$ including terms related to the asymmetry and the electric field is

$$H = BJ^2 + (A - B)J_z^2 + \frac{C - B}{4}(J_+^2 + J_-^2 + J_+J_- + J_-J_+) - \mu_p E \tag{3}$$

In an electric field, the magnetic quantum number M is the only good quantum number, and the total rotational angular momentum $\hat{J}$ is no longer conserved. States with $\pm M$ values are degenerate, and their wave functions differ by a phase of $\pi/2$ in the azimuthal angle. For the present consideration of molecular orientation, only nonnegative M values need to be considered. The nonzero terms for an asymmetric top molecule under field-free conditions are

$$H_{JKs,JKs} = \frac{B + C}{2}[J(J + 1) - K^2] + AK^2 \tag{4}$$

$$\left(\text{if } K = 1, \text{ an extra term of } (-1)^s\frac{C - B}{4}J(J + 1) \text{ needs to be added}\right)$$

$$H_{JK\pm2s,JKs} = \frac{C - B}{4}[J(J + 1) - (K \pm 1)(K \pm 2)]^{1/2} \times [J(J + 1) - K(K \pm 1)]^{1/2} \tag{5}$$

$$(\text{if } K = 0, \text{ the expression needs to be multiplied by } \sqrt{2})$$

The projection μ_A of the permanent dipole along the A axis (designated as the z direction in the molecular frame) contributes to the off-diagonal terms through

$$H_{JKs,J+1Ks} = -\frac{[(J + 1)^2 - K^2]^{1/2}[(J + 1)^2 - M^2]^{1/2}}{(J + 1)[(2J + 1)(2J + 3)]^{1/2}}\mu_A E \tag{6}$$

$$H_{JK0,JK1} = -\frac{MK}{J(J + 1)}\mu_A E \tag{7}$$

This component of the permanent dipole has a selection rule of $J_1 + J_2 + s_1 + s_2 =$ odd and $\Delta K = 0$. Contributions of the projection μ_C are (the C axis is chosen to be the x axis)

$$H_{JK+1s,JKs} = -\frac{M[(J - K)(J + K + 1)]^{1/2}}{2J(J + 1)}\mu_C E \tag{8}$$

$$H_{J+1K+1s\pm1,JKs} = \left[\frac{(J + M + 1)(J - M + 1)(J + K + 1)(J + K + 2)}{(2J + 1)(2J + 3)}\right]^{1/2} \times \frac{\mu_C E}{2(J + 1)} \tag{9}$$

$$H_{J+1K-1s\pm1,JKs} = -\left[\frac{(J + M + 1)(J - M + 1)(J - K + 1)(J - K + 2)}{(2J + 1)(2J + 3)}\right]^{1/2} \times \frac{\mu_C E}{2(J + 1)} \tag{10}$$

The selection rule is $J_1 + J_2 + s_1 + s_2 =$ even and $\Delta K = \pm 1$.

Elements related to μ_B are imaginary:

$$H_{JK+1s\pm1,JKs} = i\frac{M[(J-K)(J+K+1)]^{1/2}}{2J(J+1)}\mu_B E \quad (11)$$

$$H_{J+1K+1s,JKs} = -i\left[\frac{(J+M+1)(J-M+1)(J+K+1)(J+K+2)}{(2J+1)(2J+3)}\right]^{1/2}\times \frac{\mu_B E}{2(J+1)} \quad (12)$$

$$H_{J+1K-1s,JKs} = -i\left[\frac{(J+M+1)(J-M+1)(J-K+1)(J-K+2)}{(2J+1)(2J+3)}\right]^{1/2}\times \frac{\mu_B E}{2(J+1)} \quad (13)$$

with a selection rule of $J_1 + J_2 + s_1 + s_2 =$ odd and $\Delta K = \pm 1$. For eqs 8−13, a factor of $2^{1/2}$ needs to be multiplied whenever the term involves states with $K = 0$.

Given the elements of $\hat{H}$ in the inertial frame, calculation of the Hamiltonian $\hat{H}'$ in the dipole frame is then performed using eq 1. It is worth noting that because of the symmetry adaptation in eq 2, the rotation matrix $D(\theta_m, \varphi_m)$ in eq 1 is different from the conventional rotation matrix.[40] It is non-Hermitian, and its elements with $K_1 + K_2 + s_1 + s_2 =$ even are real, whereas those with $K_1 + K_2 + s_1 + s_2 =$ odd are imaginary. In the dipole frame, the rotational wave function is

$$|\tau M> - \sum_{J,K,s} C^{\tau,M}_{J,K,s}|JKMs>_d \quad (14)$$

where τ is a register for bookkeeping of the wave functions, and $|JKMs>_d$ are basis functions in the dipole frame. The expansion coefficients are obtained from diagonalization of the resulting Hermitian Hamiltonian using a subroutine developed at Argonne National Laboratory by Burton S. Garbow.[41]

2.2. Adiabatic and Nonadiabatic Passage. In calculating the distribution function of the permanent dipole, an angular momentum multipole expansion is used.[36,40] Distributions of the permanent dipole in the azimuthal angle φ_p have cylindrical symmetry, so only the dependence on the polar angle θ_p is relevant to this discussion. The distribution function $P(\theta_p, \varphi_p)$ is therefore expressed as

$$P(\cos\theta_p) = \int_0^{2\pi} P(\cos\theta_p, \varphi_p)\, d\varphi_p = \frac{1}{2}[1 + \sum_{n=1}^{\infty} a_n P_n(\cos\theta_p)] \quad (15)$$

where a_n represents the expansion coefficients and P_n represents Legendre polynomials. Coefficients with odd values of n represent orientation multipoles, whereas those with even values of n represent alignment. In a single-photon process using a linearly polarized laser, only the alignment coefficient a_2 can be probed. For an asymmetric top molecule with wave functions expressed as eq 14, the values of a_n can be calculated using

$$a_n = \frac{(2n+1)}{2}\sum_M N_M \sum_\tau \text{weight}(\tau M) \sum_{J_1,J_2,K,s_1,s_2} C^{\tau M*}_{J_1 K s_1} C^{\tau M}_{J_2 K s_2} \times [1 + (-1)^{s_1+s_2+J_1+J_2+n}](-1)^{M-K}\frac{[(2J_1+1)(2J_2+1)]^{1/2}}{2}\times \begin{pmatrix} J_2 & J_1 & n \\ M & -M & 0 \end{pmatrix}\begin{pmatrix} J_2 & J_1 & n \\ K & -K & 0 \end{pmatrix} \quad (16)$$

where N_M is related to the degeneracy in the electric field:

$$N_M = 2 \quad (M > 0) \qquad N_M = 1 \quad (M = 0) \quad (17)$$

and the function weight (τM) represents the population of state $|\tau M>$.

The population of each Stark level in an electric field is determined by the initial population under field-free conditions and the detailed mechanism of transformation from the field-free region to the orienting field. In a typical experimental setup, molecules coming out of a skimmer are first affected by the fringe field. As the field strength increases, Stark splittings increase. Different levels with different rotational angular momentum quantum numbers exhibit different changes in the field, and consequently, level crossings are typical. These crossings can be avoided or allowed depending on the symmetry of the involved states, and for an asymmetric top without a symmetry axis, most crossings should be avoided. At an avoided crossing, a molecular system can remain in the adiabatic path or follow a nonadiabatic passage, determined by the experimental condition and the variation of the Stark levels.[42] In general, both passages are possible. On the other hand, either adiabatic or nonadiabatic passage will inevitably result in population of some energetic metastable Stark levels. The molecules in these levels can relax through interactions with blackbody radiations or other relaxation mechanisms. The longer the residence time of these molecules in the electric field before being intercepted by a laser or another molecular beam, the more likely the relaxation. Consequently, a thermal distribution in the electric field is also a possible outcome. In the following, we consider all three scenarios in the calculation: adiabatic, nonadiabatic, and thermal distribution.

In the adiabatic calculation, we assume that all of the molecules exhibit adiabatic behavior, so the order of energy levels and the population at each level remain the same in the field as those under field-free conditions. If the energy levels are arranged in ascending order from the diagonalization procedure, the population of the ith level in the field is determined by the population of the ith level under field-free conditions. This approach is identical to that by Bulthuis et al.[36]

In the nonadiabatic calculation, we assume that the molecular system exhibits minimum changes in wave function as it traverses the fringe field and that all of the population from an initial state is transferred to a final state that is the most similar to the initial state. This is equivalent to setting all of the Landau−Zener transition probabilities to unity. The correlation between a Stark level in the field F and a level under field-free conditions is therefore established by choosing the field-free level that has the maximum overlap integral with the Stark level:

$$I_{F0} = \langle \tau_0 M_0 | \tau_F M_F \rangle \quad (18)$$

where the subscripts represent the field strengths. It is possible that the correlation is not a one-to-one correspondence; i.e., there maybe more than one Stark level that correlates with a particular level from field-free conditions. In this case, an iterative

procedure is devised: first, the field strength is decreased from F to $F1$ so that a one-to-one correlation between $|\tau_{F1}M_{F1}>$ and $|\tau_0M_0>$ can be established. Then, $|\tau_{F1}M_{F1}>$ is used to calculate the overlap integral with $|\tau_FM_F>$. If a one-to-one correlation can be established between $|\tau_{F1}M_{F1}>$ and $|\tau_FM_F>$, the correlation between $|\tau_0M_0>$ and $|\tau_FM_F>$ can thus be established. Otherwise, the field strength is again decreased from F to $F2$ for a successful correlation between $|\tau_{F1}M_{F1}>$ and $|\tau_{F2}M_{F2}>$, and the newly obtained wave functions $|\tau_{F2}M_{F2}>$ will be used to establish a correlation with $|\tau_FM_F>$. For a highly oriented system with extensive mixing of basis functions, this procedure can be time-consuming.

If the region for supersonic expansion is embedded in an electric field or if there is sufficient relaxation among the Stark levels in an electric field, a thermal population of the Stark levels may result. The weighting factor in eq 16 is thus determined by the energy of the Stark level. This scenario should correspond to the upper limit of orientation achievable using a uniform electric field, because the weighting function favors low Stark levels with oriented wave functions. In this calculation, no effect of collision-induced alignment during supersonic expansion is taken into account.[43−49]

3. Results

3.1. Distribution of Permanent Dipole. We choose two nucleic acid bases for our model calculation. Cytosine is one of the most polar species among the five bases. When using laser desorption and supersonic cooling,[50] a rotational temperature of 5 K can be expected. Adenine is the least polar base, and it is thermally stable, thus direct heating and supersonic cooling can result in a rotational temperature of 2 K.[22−29] Figure 1 shows the calculated distribution function $P(\cos\theta_p)$ of the permanent dipole of these two bases in an orienting field of 50 kV/cm. The molecular constants are shown in the insets.[51,52] The vertical axis is normalized by setting the integrated population to unity:

$$\int_0^{\pi} P(\cos\theta_p)\sin\theta_p\,d\theta_p = 1 \qquad (19)$$

and the angle θ_p represents the direction of the permanent dipole relative to the orienting field. Molecules with $\theta_p = 0°$ ($\cos\theta_p = 1$) are perfectly oriented, those with $\theta_p = 180°$ ($\cos\theta_p = -1$) are oriented backward (head and tail flipped relative to those with $\theta_p = 0°$), and those with $\theta_p = 90°$ ($\cos\theta_p = 0$) are oriented perpendicular to the electric field.

For both species, the results using the thermal approach give the highest degree of orientation, in agreement with the analysis in section 2.2. For cytosine, adiabatic calculation predicts the least degree of orientation, whereas for adenine, both adiabatic and nonadiabatic calculations result in the same degree of orientation (the two calculations are indistinguishable in the figure). It is worth noting that although cytosine has a much bigger permanent dipole than adenine, its slightly higher rotational temperature (5 K for cytosine vs 2 K for adenine) has almost canceled out all of the advantages related to the large dipole. Similar degrees of orientation are expected for the two bases.

Table 1 lists the percentage of population within a 45° cone surrounding the direction of the orienting field. The numbers are derived from Figure 1 by integrating between $\cos\theta_p = 0.707$ and 1. Compared with a randomly distributed system (field-free conditions in Table 1), the population within the 45° cone is approximately doubled due to the orienting field, even from the calculation method that predicts the least degree of orientation.

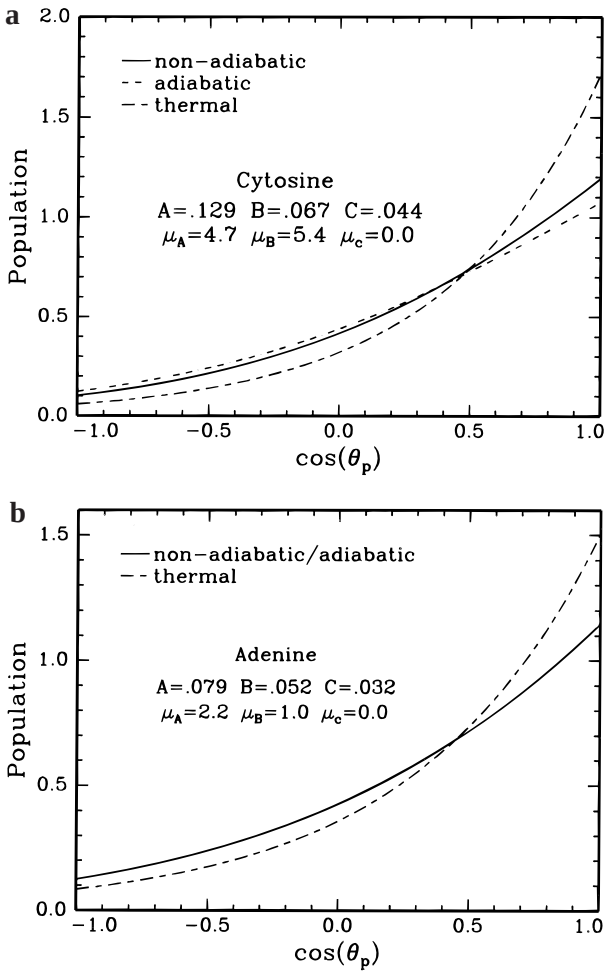

Figure 1. Distribution functions of the permanent dipole of (a) cytosine and (b) adenine in an orientation field of 50 kV/cm. The rotational temperature was 5 K for cytosine and 2 K for adenine. Rotational constants (cm^{-1}) and permanent dipoles (debye) are listed in the insets of the figure. The adiabatic and nonadiabatic calculations for adenine are indistinguishable in part b.

TABLE 1: Percentage of Molecules with Their Permanent Dipole Restricted Within 45 °C Relative to the Direction of the Orientation Field[a]

calculation	cytosine	adenine
thermal	41	37
adiabatic	29	30
non-adiabatic	32	30
field-free conditions	15	15

[a] See text for calculation details.

In our previous experiments on measurements of field-induced orientation and alignment using linearly polarized light,[22−29] we observed the variation of the efficiency of excitation. We defined a polarization ratio ρ as the ratio of excitation probabilities under perpendicular (to the electric field) and parallel excitation. If the permanent dipole is perpendicular to the transition dipole, and if the transition probability is independent of the angular momentum of the molecules (a bound-to-continuum transition), the polarization ratio is determined by

$$\rho = \frac{\int_0^{\pi} P(\cos\theta_p)\sin^2\theta_p\sin\theta_p\,d\theta_p}{\int_0^{\pi} P(\cos\theta_p)\cos^2\theta_p\sin\theta_p\,d\theta_p} \qquad (20)$$

where the factor of 2 in the denominator is because only half

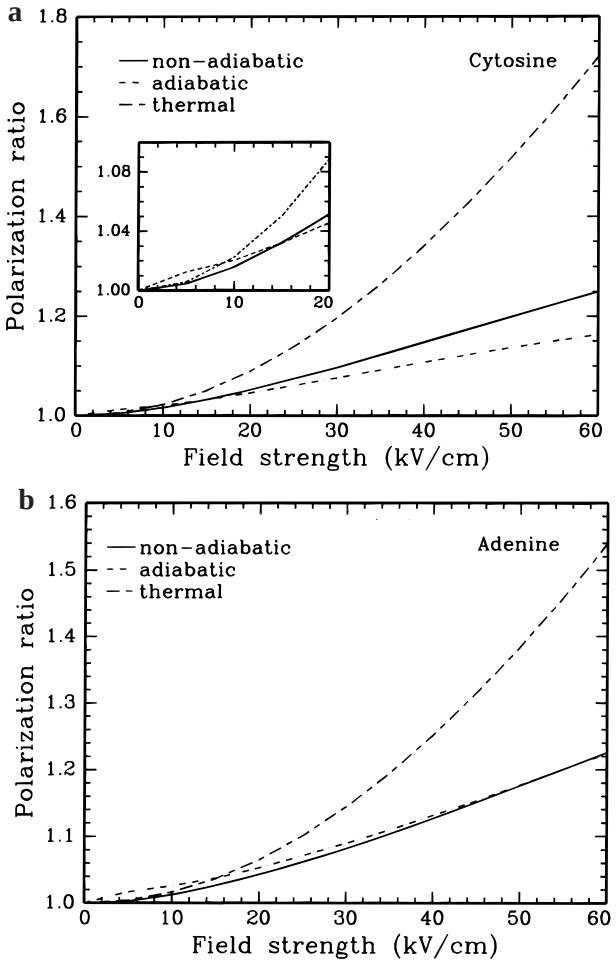

Figure 2. Polarization ratios of (a) cytosine and (b) adenine assuming the transition dipole is perpendicular to the permanent dipole. These ratios represent the enhancement in the excitation probability when the laser is polarized perpendicular, rather than parallel, to the orientation field.

of the molecules with their transition dipole in the plane perpendicular to the orienting field can be excited when the laser is polarized perpendicular to the orienting field. The value of ρ is related to the alignment multipole a_2 by

$$\rho = \frac{2a_2 + 5}{5 - a_2} \tag{21}$$

Without net alignment, $a_2 = 0$, and the polarization ratio is unity. For a more general scenario where the transition dipole is at a polar angle α from the permanent dipole, the polarization ratio is given elsewhere.[1,2] In principle, the polarization ratio should also be affected by the azimuthal angle of the transition dipole in the dipole frame, but this effect will not be considered in this context. Moreover, as will be seen in the following (section 3.3), for large systems with small rotational constants, the direction of the permanent dipole in the molecular frame has no effect on the net orientation of the molecular frame, so the azimuthal angle of the transition dipole can be set to 0, and the molecule can be assumed to rotate around the permanent dipole with cylindrical symmetry.

Figure 2 shows the variation of the polarization ratio under different orienting fields for the two bases. For cytosine at 50 kV/cm, the polarization ratio from the thermal calculation is 1.52; thus if the transition dipole is perpendicular to the permanent dipole, the excitation probability should be 52% more

TABLE 2: Orientation (a_1) and Alignment (a_2) Multipoles of Cytosine and Adenine

		cytosine			adenine		
calcn[a]		thermal	adiabatic	nonadiab.	thermal	adiabatic	nonadiab.
5	a_1	0.168[b]	0.153	0.155	0.143[b]	0.132	0.125
	a_2	0.0094	0.0209[b]	0.0077	0.0068	0.0280[b]	0.0045
10	a_1	0.333[b]	0.298	0.304	0.285[b]	0.268	0.251
	a_2	0.0373[b]	0.0338	0.0263	0.0271	0.0429[b]	0.0207
15	a_1	0.495[b]	0.426	0.440	0.424[b]	0.385	0.372
	a_2	0.0827[b]	0.0529	0.0532	0.0604	0.0617[b]	0.0435
20	a_1	0.652[b]	0.538	0.564	0.560[b]	0.493	0.484
	a_2	0.144[b]	0.0750	0.0847	0.106[b]	0.0868	0.0705

[a] In kilovolts per centimeter. [b] The largest moments obtained from the three calculation methods.

effective when the polarization direction of the excitation laser is polarized perpendicular, rather than parallel, to the orienting field. Consistent with the distribution function in Figure 1, Figure 2 also demonstrates that in general the thermal calculations give the highest ratios, corresponding to the maximum orientation effect. Under low fields (Figure 2 insets), however, the adiabatic calculations predict polarization ratios higher than those of the thermal and the nonadiabatic calculations. This can be understood from the list of orientation and alignment multipoles in Table 2. Under each orienting field, the cell containing the maximum multipole is labeled. In all cases, the thermal calculations result in the maximum orientation multipoles, but the adiabatic calculations produce the highest alignment at low fields. This is because high-energy Stark levels are more populated in the adiabatic calculation than in the thermal calculation. These levels are anti-oriented relative to the electric field, so the net orientation is smaller but the net alignment is higher in the adiabatic calculation. As the field strength increases, better orientation induces better alignment, so the relative contribution from the anti-oriented molecules becomes less important, and the thermal calculation produces the highest orientation and alignment factors. Because the polarization ratio is only related to the alignment multipole a_2, it is therefore no surprise that Figure 2 exhibits a different ordering of the polarization ratios in low fields. It is interesting to notice that for adenine, the adiabatic and nonadiabatic calculations switch order between 50 and 60 kV/cm, so the distribution functions from the two calculations in Figure 1a are indistinguishable.

Experimental measurements of the distribution function of the permanent dipole have been accomplished through bound-to-continuum transitions in ICl by Vigué's group[21] and in ICN,[23,27,28] BrCN,[25,28] and *tert*-butyl nitrite[29] by our group. For example, the transition dipole of the S_1 state of *tert*-butyl nitrite is known to be perpendicular to the O−N═O plane,[53] whereas the permanent dipole is in the O−N═O plane. Under perpendicular excitation, the excitation probability and thereby the yield of the NO photoproduct should be enhanced compared with those under parallel excitation. Figure 3 shows the experimental polarization ratios from the R_1 (9.5)/P_1 (24.5) transition of NO at a dissociation wavelength of 365.8 nm.[29] The uncertainty is mainly related to the instability of the molecular beam, fluctuations in the laser power, and nonuniformity of the laser beam. Overlaid are calculation results using the above three approaches assuming a permanent dipole of 2.77 D (along the *A* axis) and rotational constants of $A = 0.1468$ cm^{-1}, $B = 0.0576$ cm^{-1}, and $C = 0.0572$ cm^{-1}.[54,55] The rotational temperature was assumed to be 2 K, determined from a series of experiments.[22−29] Under low fields (below 20 kV/cm), all three calculations predict similar polarization ratios, and within the

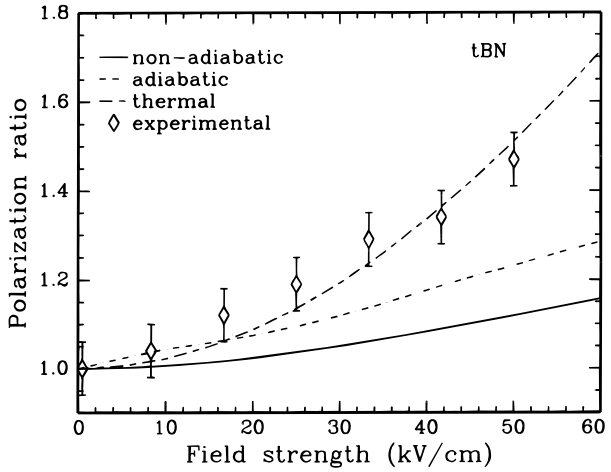

Figure 3. Polarization ratios of NO from photodissociation of oriented *tert*-butyl nitrite. The vertical axis represents the ratio of the yields of NO when the dissociation laser was polarized perpendicular and parallel to the orientation field.

error limit, they all agree with the experimental data. However, under high fields, the best agreement with experiment is obtained using the thermal calculation, rather than the adiabatic or the nonadiabatic approaches. Similar conclusions are consistently obtained in other bound-to-continuum and bound-to-bound transitions (next section). The population distribution in the Stark field from our experimental apparatus therefore resembles a thermal distribution, and the resulting orientation is more effective than the predictions using the adiabatic or the nonadiabatic approaches. We attribute this result to effective relaxation of the high-energy Stark levels in the field and perhaps additional alignment caused by the supersonic expansion,[43−49] although our preliminary attempts at probing this collision-induced alignment in the molecular beam are unsuccessful to date.

3.2. Spectroscopic Details. For a more detailed comparison between theory and experiment, we investigate the spectroscopic features of a partially resolved bound-to-bound transition. The transition intensity distribution is calculated using

$$I_{\tau_2 M_2 \leftarrow \tau_1 M_1} \propto \sum_p N_{M_1} \,\mathrm{weight}(\tau_1 M_1) \left| \sum_{J_2 K_2 S_2, J_1 K_1 S_1} \frac{1}{2} C^{\tau_2 M_2}_{J_2 K_2 S_2} C^{\tau_1 M_1 *}_{J_1 K_1 S_1} (-1)^{M_1 - K_1} \times \sum_q \mu_t(1,q) E(1,p) (-1)^{p-q} \begin{pmatrix} J_1 & J_2 & 1 \\ -M_1 & M_2 & -p \end{pmatrix} \times \left[\begin{pmatrix} J_1 & J_2 & 1 \\ -K_1 & K_2 & q \end{pmatrix} + (-1)^{s_1} \begin{pmatrix} J_1 & J_2 & 1 \\ K_1 & K_2 & q \end{pmatrix} \right] [(-1)^{s_1+s_2+J_1+J_2} + 1] \times [(2J_1+1)(2J_2+1)]^{1/2} \right|^2 \quad (22)$$

It is worth noting that in the above equation the molecular frame should remain identical for both the lower and upper state of the transition; i.e., the same rotation matrix $D(\theta_m, \varphi_m)$ should be used for the Hamiltonian matrix of both states, and the transition dipole should also be expressed in the dipole frame. Figure 4 shows the $\pi^* \leftarrow n$ transition of pyrimidine recorded in a field of 50 kV/cm.[26] The two panels represent the two polarization directions of the resonant laser in the REMPI experiment. The same plotting scale is used for both panels, and for each calculation method, the same scaling factor is used for both polarization directions. However, different calculation methods require different scaling factors because of the difference in the effective rotational partition function. The two spectra from adiabatic and nonadiabatic calculations are very similar on the low-energy side, but they are noticeably different from the thermal calculation. Above 310 71 cm^{-1}, all three calculations are similar in intensity distributions, and they are all in agreement with the experimental data. Below 31 070 cm^{-1}, the thermal calculations show better agreement with the experiment than the adiabatic and nonadiabatic calculations, whereas between 31 070 and 31 071 cm^{-1}, the adiabatic and nonadiabatic calculations show better resemblance of the experimental spectra. Overall, the agreement with experimental spectra is similar for all three calculations, and higher quality experimental data are necessary to clarify this comparison.

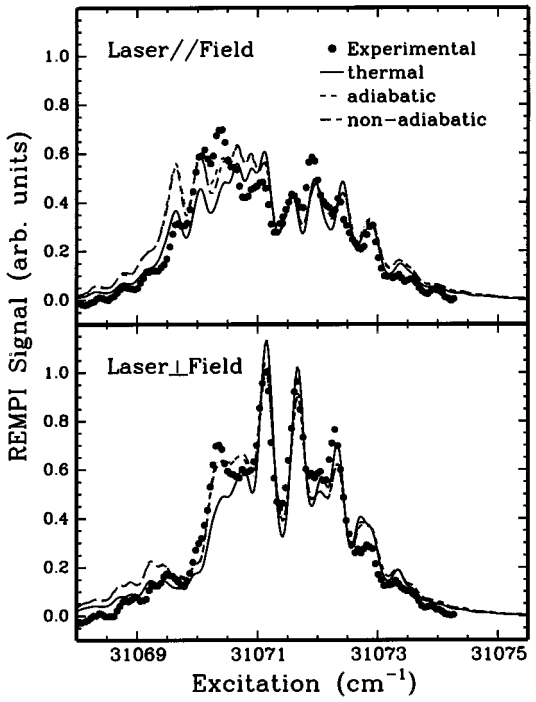

Figure 4. REMPI spectra of pyrimidine in an orientation field of 50 kV/cm. The top (bottom) panel corresponds to the resonant laser polarized parallel (perpendicular) to the orientation field.

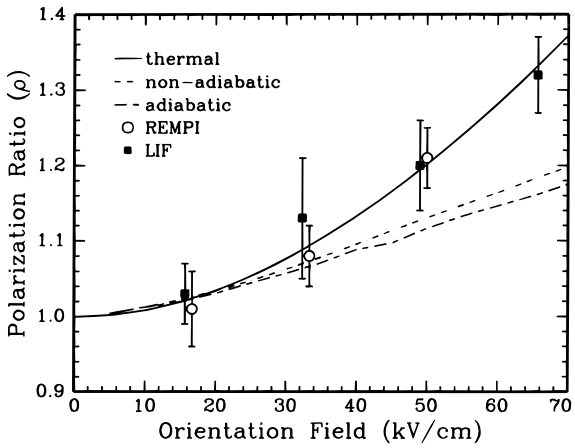

Figure 5. Polarization ratios from REMPI and LIF of pyrimidine. The experimental values were obtained by taking the ratios of the integrated spectra under the two different polarizations of the resonant laser. The horizontal scale of the LIF data is shifted by −1 kV/cm for clarity.

The polarization ratio in this context is defined as the ratio between the overall spectral intensity under perpendicular and parallel excitation. Figure 5 shows the experimental and calculation results. Similar to section 3.1, under high fields, the

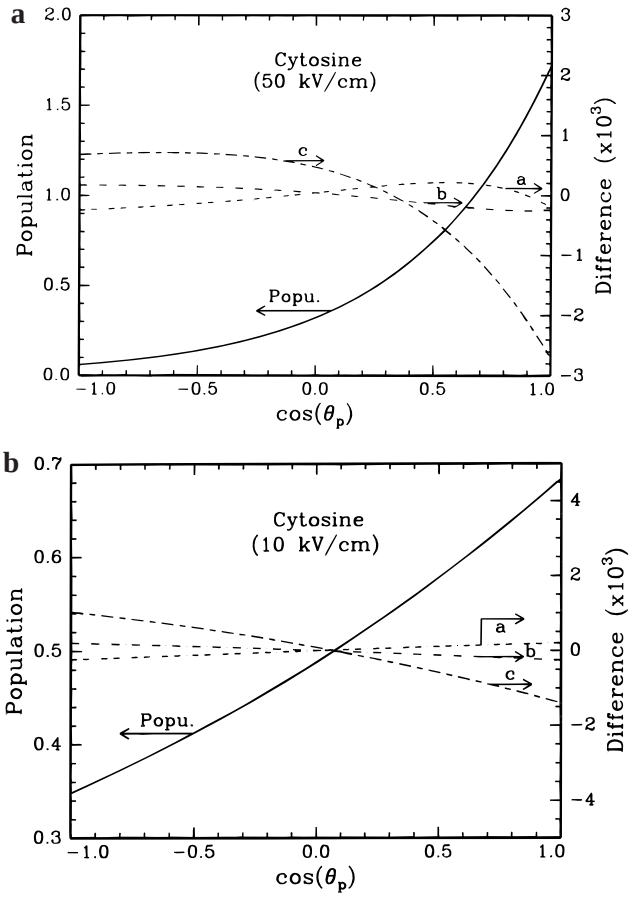

Figure 6. Distribution functions of the permanent dipole in orientation fields of (a) 50 and (b) 10 kV/cm. The solid line represents the result using the permanent dipole listed in Figure 1a. The dashed lines are differences between the solid line and calculation results assuming the permanent dipole along the (a) *A*, (b) *B*, and (c) *C* principal axes. The vertical scale of the "difference" curves is on the right of the figure. For all calculations, the size of the permanent dipole remained the same.

experimental data is better represented by the thermal calculation than either the adiabatic or the nonadiabatic calculations. It is therefore implied that the population inversion among Stark levels resulting from adiabatic or nonadiabatic passages may have been effectively relaxed to a more or less thermal distribution under our experimental conditions. It is worth noting that by lowering the rotational temperature the results in Figure 5 could be changed. However, pyrimidine has well-resolved rovibronic transitions under field-free conditions, so the rotational temperature of the molecular beam is not an adjustable parameter in this case.

3.3. Effects of Rotational Constants and Permanent Dipoles on Orientation. A challenge in the investigation of polarization directions of electronic transitions in biomolecules is posed by the lack of spectroscopic data, including rotational constants and permanent dipoles. In this section, we investigate sensitivities of orientation on molecular parameters, including rotational constants and the direction of the permanent dipole in the molecular frame. The rotational temperature and the size of the permanent dipole are fixed, and the distribution functions of the permanent dipole are calculated by assuming different orientations of the permanent dipole in the molecular frame and different rotational constants.

Figure 6 shows the resulting distribution functions of cytosine in orienting fields of 10 and 50 kV/cm from the thermal calculation. The rotational constants and temperatures are the same as those in Figure 1a. The solid lines present the distribution function obtained using the orientation of the permanent dipole given in Figure 1a. Results assuming the permanent dipole along the *A*, *B*, and *C* axes are so similar to the solid line that only the differences are plotted as the dashed lines labeled *a*, *b*, and *c* respectively. The vertical scale for the dashed lines is labeled on the right. Figure 6 suggests that the net orientation is independent of the detailed shape of the molecule, even under low field strengths. As long as the overall size of the permanent dipole and the rotational temperature of the molecular beam are known, the distribution function of the permanent dipole can be calculated.[33] Furthermore, for simplicity in calculation, the permanent dipole can be assumed to be along any principal axis. The polarization ratio is thus not a sensitive measure of the direction of the permanent dipole, although it is a convenient and sensitive measure of the direction of a transition dipole relative to the permanent dipole.[25,26]

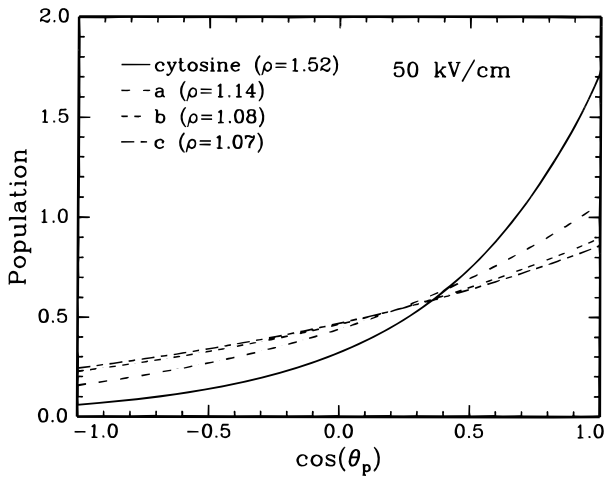

Figure 7. Distribution functions of the permanent dipole in an orientation field of 50 kV/cm. The solid line is a reproduction of the distribution function in Figure 6a. The dashed lines are results assuming rotational constants 2 orders of magnitude larger than those given in Figure 1a: $A = 12.9$, $B = 6.7$, and $C = 4.4$ cm^{-1}. The permanent dipole is 7.16 debye, identical for all of the calculations, and it is oriented along the (a) *A*, (b) *B*, or (c) *C* axis.

The above result can be understood from the following consideration:[56] orientation is a result of suppression of molecular rotation. The suppressive force is determined by the size of the permanent dipole and the strength of the electric field, whereas the rotational energy ($3k_BT/2$ in classical mechanics) is determined by the rotational temperature. From a classical point of view, the detailed mass distribution in the molecular frame should therefore not affect the balance between orientation and rotation. In fact, the multipoles obtained from the thermal calculation listed in Table 2 are almost identical to those obtained using the classical Debye formulas.[57]

From a quantum mechanical point of view, however, the above result should be due to the small rotational constants of cytosine, which result in closely spaced energy levels almost describable using classical mechanics. A more dramatic dependence on the direction of the permanent dipole in the molecular frame should be observable for systems with larger rotational constants. Figure 7 shows the distribution functions calculated using rotational constants 2 orders of magnitude larger than those given in Figure 1a. For comparison, the distribution function in Figure 6a is also reproduced. The dashed lines labeled a, b, and c are distribution functions assuming the increased rotational constants and a permanent dipole along the *A*, *B*, or *C* axis, respectively. The expected polarization ratios ρ are also listed

in each case. For this hypothetical molecular system with the increased rotational constants, the sensitivity of orientation on the direction of the permanent dipole is indeed greatly enhanced, and the resulting variation of the polarization ratio ranges from 1.14 to 1.07. The most effective orientation is achieved when the permanent dipole is along the *A* axis, while the least is obtained when the dipole is along the *C* axis. In addition, the orientation achieved with the enlarged rotational constants is much less compared with that of the original cytosine system. The polarization ratio is decreased by ~30%! This deterioration in orientation is related to the decrease in the number of pendular states due to large energy separations between the quantum states. Fortunately, all biomolecules have small rotational constants, so the lack of knowledge on the direction of the permanent dipole or the precise rotational constants should not hinder theoretical predictions of the field-induced orientation effect.

4. Conclusion

We have calculated the distribution functions of the permanent dipole in a uniform electric field for an asymmetric top with its permanent dipole not parallel to any principal axis. In a field of 50 kV/cm, for cytosine at 5 K and for adenine at 2 K, more than 30% of the population is calculated to be confined within a 45° cone. If probed using a linearly polarized laser and if the transition dipole is perpendicular to the permanent dipole, the excitation probability should be enhanced by 50% when the excitation laser is polarized perpendicular to the orienting field. Effective orientation is achieved for relatively large systems with small rotational constants. The resulting net orientation in large molecules is independent of the direction of the permanent dipole in the molecular frame, so even for systems that are not well-known spectroscopically, the distribution function of the permanent dipole can still be estimated, as long as the size of the permanent dipole and the rotational temperature are known. However, for small molecules with large rotational constants, quantum effects become prominent, and the orientation effect shows dependence on the orientation of the permanent dipole in the molecular frame.

Among the three models of calculation, the thermal distribution gives the highest degree of orientation, and the polarization ratios from both bound-to-bound and bound-to-continuum transitions are in agreement with available experimental data. The adiabatic and nonadiabatic approaches predict lower extent of orientation than the experiment. A likely reason for this discrepancy might be effective relaxation from the upper Stark levels populated during the adiabatic or nonadiabatic passage. Detailed spectroscopic comparisons in pyrimidine, however, are inconclusive. Higher quality experimental data will help clarify this point.

Acknowledgment. W.K. is grateful for assistance from Dr. P. H. Vaccaro (Yale University) on the nonadiabatic calculation method and Dr. H. Guo (University of New Mexico) for suggestions regarding programming details. J.B. acknowledges valuable discussions with Dr. G. van der Zwan. The authors thank Karen J. Castle (Oregon State University) for proofreading the manuscript. This project is supported by the National Science Foundation, Division of Chemistry, through the Faculty Early Career Development Program.

References and Notes

(1) Block, P. A.; Bohac, E. J.; Miller, R. E. *Phys. Rev. Lett.* **1992**, *68*, 1303.
(2) Bemish, R. J.; Bohac, E. J.; Wu, M.; Miller, R. E. *J. Chem. Phys.* **1994**, *101*, 9457.
(3) Oudejans, L.; Miller, R. E. *J. Phys. Chem.* **1995**, *99*, 13670.
(4) Bemish, R. J.; Chan, M. C.; Miller, R. E. *Chem. Phys. Lett.* **1996**, *251*, 182.
(5) Oudejans, L.; Miller, R. E. *J. Phys. Chem.* **1997**, *101*, 7582.
(6) Oudejans, L.; Moore, D. T.; Miller, R. E. *J. Chem. Phys.* **1999**, *110*, 209.
(7) Oudejans, L.; Miller, R. E. *J. Phys. Chem.* **1999**, *103*, 4791.
(8) Loesch, H. J.; Remscheid, A. *J. Chem. Phys.* **1990**, *93*, 4779.
(9) Loesch, H. J.; Remscheid, A. *J. Phys. Chem.* **1991**, *95*, 8194.
(10) Loesch, H. J.; Möller, J. *J. Chem. Phys.* **1992**, *97*, 9016.
(11) Loesch, H. J.; Möller, J. *J. Phys. Chem.* **1993**, *97*, 2158.
(12) Van Leuken, J. J.; Bulthuis, J.; Stolte, S.; Loesch, H. J. *J. Phys. Chem.* **1995**, *99*, 13582.
(13) Loesch, H. J.; Möller, J. *J. Phys. Chem. A* **1997**, *101*, 7534.
(14) Loesch, H. J.; Möller, J. *J. Phys. Chem. A* **1998**, *102*, 9410.
(15) Friedrich, B.; Rubahn, H.-G.; Sathyamurthy, N. *Phys. Rev. Lett.* **1992**, *69*, 2487.
(16) Friedrich, B.; Herschbach, D. R.; Rost, J.-M.; Rubahn, H.-G.; Renger, M.; Verbeek, M. *J. Chem. Soc., Faraday Trans.* **1993**, *89*, 1539.
(17) Slenczka, A.; Friedrich, B.; Herschbach, D. *Chem. Phys. Lett.* **1994**, *224*, 238.
(18) Friedrich, B.; Slenczka, A.; Herschbach, D. *Chem. Phys. Lett.* **1994**, *221*, 333.
(19) Durand, A.; Loison, J. C.; Vigué, J. *J. Chem. Phys.* **1994**, *101*, 3514.
(20) Bazalgette, G.; White, R.; Loison, J. C.; Trénec, G.; Vigué, J. *Chem. Phys. Lett.* **1995**, *244*, 195.
(21) Bazalgette, G.; White, R.; Trénec, G.; Audouard, E.; Büchner, M.; Vigué, J. *J. Phys. Chem. A* **1998**, *102*, 1098.
(22) Li, H.; Franks, K. J.; Hanson, R. J.; Kong, W. *Proceedings of SPIE* **1998**, *3271*, 142.
(23) Franks, K. J.; Li, H.; Hanson, R. J.; Kong, W. *J. Phys. Chem.* **1998**, *102*, 7881.
(24) Li, H.; Franks, K. J.; Hanson, R. J.; Kong, W. *J. Phys. Chem.* **1998**, *102*, 8084.
(25) Franks, K. J.; Li, H.; Kong, W. *J. Chem. Phys.* **1999**, *110*, 11779.
(26) Franks, K. J.; Li, H.; Kong, W. *J. Chem. Phys.* **1999**, *111*, 1884.
(27) Li, H.; Franks, K. J.; Kong, W. *Chem. Phys. Lett.* **1999**, *300*, 247.
(28) Franks, K. J.; Li, H.; Kuy, S.; Kong, W. *Chem. Phys. Lett.* **1999**, *302*, 151.
(29) Franks, K. J.; Kong, W. *J. Chem. Phys.* **1999**, submitted for publication.
(30) Wang, S.-X.; Booth, J. L.; Dalby, F. W.; Ozier, I. *J. Chem. Phys.* **1994**, *101*, 5464.
(31) Friedrich, B.; Herschbach, D. R. *Nature* **1991**, *353*, 412.
(32) Friedrich, B.; Herschbach, D. R. *Z. Phys.* D **1991**, *18*, 153.
(33) Stolte, S. *Nature* **1991**, *353*, 391.
(34) Rost, J. M.; Griffin, J. C.; Friedrich, B.; Herschbach, D. R. *Phys. Rev. Lett.* **1992**, *68*, 1299.
(35) Loesch, H. J. *Annu. Rev. Phys. Chem.* **1995**, *46*, 555.
(36) Bulthuis, J.; Möller, J.; Loesch, H. J. *J. Phys. Chem. A* **1997**, *101*, 7684.
(37) Moore, D. T.; Oudejans, L.; Miller, R. E. *J. Chem. Phys.* **1999**, *110*, 197.
(38) Loison, J. C.; Durand, A.; Bazalgette, G.; White, R.; Audouard, E.; Vigué, J. *J. Phys. Chem.* **1995**, *99*, 13591.
(39) Choi, S. E.; Bernstein, R. B. *J. Chem. Phys.* **1986**, *85*, 150.
(40) Zare, R. N. *Angular Momentum*; Wiley-Interscience: New York, 1988.
(41) Garbow, B. S. http://www.netlib.org/cgi-bin/netlibget.pl/eispack/ch.f.
(42) Landau, L. D.; Lifschitz, E. M. *Course of Theoretical Physics, Vol. 3, Quantum Mechanics*, 3rd ed.; Pergamon Press: Oxford, 1977; Chapter XI.
(43) Pullman, D. P.; Friedrich, B.; Herschbach, D. R. *J. Chem. Phys.* **1990**, *93*, 3224.
(44) Pullman, D. P.; Friedrich, B.; Herschbach, D. R. *J. Phys. Chem.* **1995**, *99*, 7407.
(45) Neitzke, H.-P.; Terlutter, R. *J. Phys. B* **1992**, *25*, 1931.
(46) Saleh, H. J.; McCaffery, A. J. *J. Chem. Soc., Faraday Trans.* **1993**, *89*, 3217.
(47) Aquilanti, V.; Ascenzi, D.; Cappelletti, D.; Pirani, F. *Nature* **1994**, *371*, 399.
(48) Weida, M. J.; Nesbitt, D. J.; *J. Chem. Phys.* **1994**, *100*, 6372.
(49) Harich, S.; Wodtke, A. M. *J. Chem. Phys.* **1997**, *107*, 5983.
(50) Meijer, G.; Berden, G.; Leo Meerts, W.; Hunziker, H. E.; de Vries, M. S.; Wendt, H. R. *Chem. Phys.* **1992**, *163*, 209.
(51) Brown, R. D.; Godfrey, P. D.; McNaughton, D.; Pierlot, A. P. *Chem. Phys. Lett.* **1989**, *156*, 61.
(52) Brown, R. D.; Godfrey, P. D.; McNaughton, D.; Pierlot, A. P. *J. Am. Chem. Soc.* **1989**, *111*, 2309.

(53) Schwartz-Lavi, D.; Rosenwaks, S. *J. Chem. Phys*. **1988**, *88*, 6922.
(54) Gray, P.; Pearson, M. J. *Trans. Faraday Soc.* **1963**, *59*, 347.
(55) Heineking, N.; Jäger, W.; Gerry, M. C. L. *J. Mol. Spec*. **1992**, *155*, 403.
(56) Friedrich, B.; Herschbach, D. *Intern. Rev. Phys. Chem*. **1996**, *15*, 325.
(57) Atkins, P. W. *Molecular Quantum Mechanics*, 2nd ed.; Oxford University Press: Oxford, 1983; p 357.